

Stability of the Cationic Oxidation States in $\text{Pr}_{0.50}\text{Sr}_{0.50}\text{CoO}_3$ across the Magnetostructural Transition by X-ray Absorption Spectroscopy

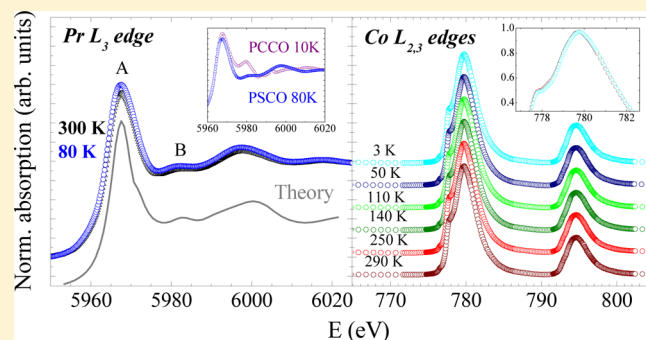
Jessica Padilla-Pantoja,^{*,†} Javier Herrero-Martín,[‡] Pierluigi Gargiani,[‡] S. Manuel Valvidares,[‡] Vera Cuartero,^{‡,§} Kurt Kummer,[§] Oliver Watson,[§] Nicholas B. Brookes,[§] and José Luis García-Muñoz[†]

[†]Institut de Ciència de Materials de Barcelona, ICMA-B-CSIC, Campus universitari de Bellaterra, E-08193 Bellaterra, Barcelona, Spain

[‡]ALBA Synchrotron, 08290 Cerdanyola del Vallès, Barcelona, Spain

[§]European Synchrotron Radiation Facility, F-38043 Grenoble Cedex 9, France

ABSTRACT: The possible hybridization between Pr 4f and O 2p states in $\text{Pr}_{0.50}\text{Sr}_{0.50}\text{CoO}_3$ at low temperatures was investigated by different techniques. First, using neutron diffraction we observed a strong contraction of some Pr–O bonds across the magnetostructural transition at $T_S \sim 120$ K. In contrast to the Pr–O bond contraction in $\text{Pr}_{0.50}\text{Ca}_{0.50}\text{CoO}_3$, this transition is not accompanied by the appearance of Pr^{4+} at low temperatures, as revealed by X-ray absorption spectroscopy at Pr edges. Despite the fact that a Pr valence change is not the mechanism that drives this transition, we point out an active participation of Pr ions across T_S . Moreover, Co $L_{2,3}$ -edge and O K edge X-ray absorption spectra did not reveal any spin-state variation and showed the stability of the average formal valence of cobalt ions. The large density of empty t_{2g} symmetry states in the studied thermal range does not suggest the occurrence of Co^{3+} in a pure low-spin state. The overall metallic behavior agrees with our findings. We propose a mixture of Co^{3+} ions in the intermediate-spin or high-spin configuration together with Co^{4+} ions in a low- or intermediate-spin state.



INTRODUCTION

The electronic and magnetic properties of cobalt-based perovskites are largely determined by the electronic filling of the Co 3d valence band. The spin state of trivalent cobalt appears as a fundamental ingredient for the variety of magnetic and electronic properties displayed by the $(\text{Ln}_{1-y}\text{Ln}'_y)_{1-x}\text{A}_x\text{CoO}_3$ (Ln, Ln' = lanthanide; A = alkaline-earth) family of compounds.^{1–4} In particular, the physical properties of half-doped $\text{Pr}_{0.50}\text{A}_{0.50}\text{CoO}_3$ (A = Ca, Sr) perovskites are attracting interest because of the observation of nonconventional phase transitions and distinct structural and magnetic properties.^{5–14}

Half-doped $\text{Pr}_{0.50}\text{Ca}_{0.50}\text{CoO}_3$ (PCCO) is metallic, but a metal–insulator (MI) transition localizes the mobile charges below $T_{\text{MI}} \sim 80$ K, assisted by concomitant Co spin-state changes that favor the diamagnetic Co^{3+} low-spin (LS) state, which explains the absence of long-range magnetic order.^{1,3–9} The correct picture for this transition was a long-standing open question until the discovery that the extra tilting of CoO_6 octahedra (compatible with the $Pnma$ crystal symmetry of PCCO) is activated by a contraction of selected Pr–O bonds^{5,7,8} that generates a first-order Pr^{3+} to Pr^{4+} valence shift at T_{MI} . This exceptional electronic mechanism in PCCO and other $(\text{Pr,Ln})_{1-x}\text{Ca}_x\text{CoO}_3$ cobaltites implies that the insulating state is stabilized by electron transfer from Pr to Co sites.^{6–9}

$\text{Pr}_{0.50}\text{Sr}_{0.50}\text{CoO}_3$ (PSCO) exhibits ferromagnetic (FM) order below $T_C \sim 230$ K and metallic conductivity over the whole temperature range. In addition, it undergoes an intriguing magnetostructural transition at $T_S \sim 120$ K.^{10–14} This unexpected transition was initially reported by Mahendiran and Schiffer¹⁰ on the basis of magnetic measurements and confirmed later by other groups. It causes an unusual steplike behavior in the magnetization and presumably a change of the magnetic easy axis.¹⁵ Thus, the transition brings about an anomalous magnetic field dependence of the steplike change in $M(T)$ at T_S , where the magnetization decreases or increases depending on the magnitude of the applied field.^{10–12} Troyanchuk et al.¹³ found evidence of structural anomalies, and several groups (using different structural descriptions) have underlined the possible importance of the Pr 4f–O 2p hybridization for this transition.^{11,13} Other different hypothetical pictures have been also invoked (orbital ordering or orbital state changes, spin-state changes in Co^{3+} ions, etc.) without any conclusive result.

The unexpected transition at $T_S \sim 120$ K has not been observed with other rare-earth cations. It does not appear in $\text{Nd}_{0.5}\text{Sr}_{0.5}\text{CoO}_3$ ¹⁶ or $(\text{La}_{1/3}\text{Nd}_{2/3})_{0.50}\text{Sr}_{0.50}\text{CoO}_3$,¹⁷ and Leighton et al.¹¹ reported the disappearance of the transition when La replaces Pr as in $(\text{La}_{1-y}\text{Pr}_y)_{0.5}\text{Sr}_{0.5}\text{CoO}_3$. Interestingly, they

Received: December 20, 2013

Published: August 11, 2014

reported that the presence of even a small Pr concentration (~5% of A-site occupation) is enough to activate the effects. The absence of this transition in other half-doped cobaltites without Pr ions can be a signature of a dominant role for Pr–O hybridization in the structural and magnetocrystalline anisotropy changes. Furthermore, the spontaneous Pr valence shift reported in PCCO and other $(\text{Pr}_x\text{Ln}_{1-x})\text{Ca}_x\text{CoO}_3$ cobaltites justifies similar exploratory studies across the coupled structural/magnetocrystalline anisotropy transition in PSCO. This provides the motivation to study the temperature evolution of experimental X-ray absorption spectra at the Pr $M_{4,5}$ and Pr L_3 edges in $\text{Pr}_{0.5}\text{Sr}_{0.5}\text{CoO}_3$ and to compare them to the results of theoretical calculations. In the present study, we observed minor changes across T_S , allowing us to conclude the absence of Pr^{4+} . Moreover, we checked for possible spin-state variations by looking at the Co $L_{2,3}$ and O K edges. Our results demonstrate that both the average valence and spin state of Co ions remain unaltered across the anomalous transitions.

EXPERIMENTAL SECTION

Polycrystalline PSCO powder was prepared by solid-state reaction under an oxygen atmosphere. High-purity Co_3O_4 and Pr_6O_{11} oxides were first dried at 1100°C for 15 h. SrCO_3 was heated at 850°C for 12 h and then to 950°C for 15 h to decompose calcium carbonate. The precursors were mixed in stoichiometric amounts. The mixture was pressed into pellets, heated under an oxygen atmosphere at 1000°C for 12 h, and then slowly cooled ($60^\circ\text{C}/\text{h}$). After the sample was grinded and pressed, the last two annealings were performed at 1100°C for 12 h and 1170°C for 24 h under O_2 , also using slow cooling.

Sample quality was checked by powder X-ray diffraction using a Siemens D-5000 diffractometer. The material was found to be single-phase and free from impurities. The direct current (dc) magnetization was measured using a superconducting quantum interferometer device (SQUID) (Quantum Design) under 0.1 mT. The evolution of the ferromagnetic response below T_C is shown in Figure 1a, where the

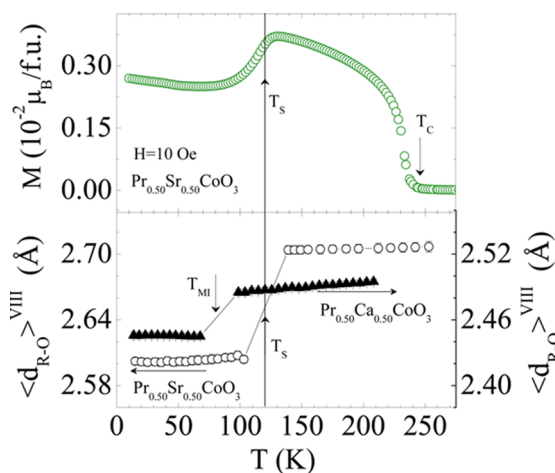


Figure 1. (Top) Temperature dependence of the dc magnetization at low field in $\text{Pr}_{0.5}\text{Sr}_{0.5}\text{CoO}_3$ (field-cooled, 0.1 mT), signaling the second transition (T_S) well below T_C . (Bottom) Comparison of the thermal evolutions of the average $\langle(\text{Pr,A})\text{--O}\rangle$ bond distances (VIII-coord.) in $\text{Pr}_{0.5}\text{Sr}_{0.5}\text{CoO}_3$ (left axis) and $\text{Pr}_{0.5}\text{Ca}_{0.5}\text{CoO}_3$ (right axis).

apparent drop in the magnetization at around $T_S \sim 120$ K corresponds to the magnetocrystalline transition into the low-temperature phase. The steplike behavior in the magnetization has been attributed to possible changes in the magnetocrystalline anisotropy axis.^{11,12} Sample characterization included powder neutron diffraction measurements using D20 at Institut Laue-Langevin (Grenoble, France) with $\lambda = 1.87$ Å. The structural model of ref 11 was used to fit the diffraction data at

low temperature. We detected a contraction of the cell volume in PSCO at $T < T_S$.¹⁷ In order to get further insight into possible changes in the hybridization of Pr–O bonds, we analyzed the average R–O bond distances on both sides of the magnetocrystalline transition in our PSCO sample¹⁷ (see Figure 1b). We recall the evolution of Pr–O bonds in PCCO across T_{MI} from refs 8, 11, and 17. Using these previously reported data, in Figure 1b we show a comparison of the evolution of the $\langle(\text{R--O})^{\text{VIII}}\rangle$ distance (considering the nearest eight oxygens of the 12-fold coordination sphere around Pr) in the half-doped cobaltites $\text{Pr}_{0.5}\text{A}_{0.5}\text{CoO}_3$ ($\text{A} = \text{Ca}, \text{Sr}$). This average bond length contracts markedly in PSCO at T_S (ca. –4%). In contrast, the variations of this parameter in PCCO (which contains tetravalent Pr ions at low temperatures) across T_{MI} are smaller. It is also noteworthy that the unit-cell volume contraction with Ca is one order of magnitude larger than in the Sr perovskite because of a strong expansion of the four (out of 12) longest Pr–O bonds below T_S in the latter.¹⁷ This finding gives support to the observations made in the Introduction of this paper about the need to clarify the role of Pr and the Pr–O hybridization in PSCO, in particular the temperature dependence of the Pr oxidation state across T_S .

Soft X-ray absorption spectroscopy (XAS) measurements at the Pr $M_{4,5}$, O K, and Co $L_{2,3}$ edges were performed on the BL29-BOREAS beamline at the ALBA Synchrotron and on beamline ID08 at the ESRF. Data were recorded by means of surface-sensitive total electron yield and total fluorescence yield. Proper bulk-pellet-sensitive measurements required in situ cleaving of the samples under ultrahigh vacuum ($\sim 10^{-9}$ mbar) conditions. CoO was simultaneously measured as an energy calibration reference. The nominal flux on the BL29-BOREAS beamline was on the order of 10^{12} photons/s with an energy resolution of about 50 meV. Flux and time exposure were selectively reduced in some cases in order to minimize photoreduction of Co ions.

Additional Pr L_3 -edge XAS measurements were recorded in transmission on the BL22-CLÆSS beamline at the ALBA Synchrotron Light Facility. The measurements were carried out on pellets made of fine powders of the material homogeneously mixed with cellulose. The thickness of the pellets was optimized for transmission measurements to get an edge step close to 1. The energy calibration was simultaneously done by performing measurements on a Cr foil (Cr K edge, 5989 eV). A Si stripe was selected on the white beam mirror to remove higher-order harmonics. The incident beam was defocused, and the spot size was $1.0 \text{ mm} \times 0.7 \text{ mm}$ (height \times width). A Si(111) double-crystal monochromator was used to get ~ 1 eV energy resolution at 6 keV with approximately 10^{12} photons/s.

RESULTS AND DISCUSSION

A. XAS at the Pr $M_{4,5}$ and Pr L_3 Edges. Figure 2 shows the experimental X-ray absorption spectra of PSCO at the Pr $M_{4,5}$ edges recorded at different temperatures between 10 and 340 K. For comparison, we have also plotted the corresponding spectra of PCCO at room temperature (RT) and 10 K (from ref 9) and that of PrCoO_3 (PCO) at 300 K as a Pr^{3+} reference compound. Figure 2 shows hardly any change in the PSCO spectrum over the whole thermal range studied, which includes T_C and T_S . Moreover, the PCCO spectrum at 300 K shows a remarkable similarity to the PSCO spectra. We found only some dissimilarities in the $M_{4,5}$ branching ratio, which is defined as $I(M_5)/[I(M_4) + I(M_5)]$, where I is the measured absorption intensity. These are probably due to small differences in the spin–orbit splitting.¹⁸ We found $M_{4,5}$ branching ratio values of 0.582 and 0.589 for PCCO at 10 and 300 K, respectively. Meanwhile, this parameter is within 0.600 and 0.598 for PSCO at all temperatures between 10 and 340 K. As a reference, we also experimentally found a branching ratio of 0.646 for PCO at 300 K. The general trend of the $M_{4,5}$ branching ratio in lanthanides is directly proportional to the occupation of the 4f

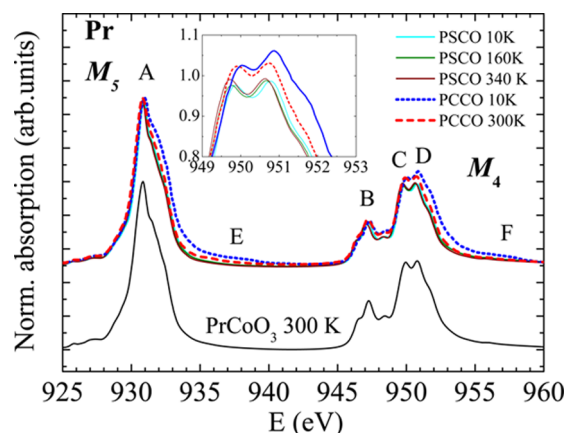


Figure 2. Experimental Pr $M_{4,5}$ -edge XAS spectra of PSCO as a function of temperature. For comparison, the spectra of PCCO at 10 K (blue dotted) and 300 K (red dashed) are also shown. The black line is the experimental spectrum of PrCoO_3 at 80 K as a reference sample. A, B, C, D, E, and F are labels for spectroscopic features. The inset shows details of the Pr M_4 edge.

orbitals because of a progressively less prominent M_4 edge,¹⁹ which is in qualitative agreement with the values we found.

Although the Pr ions in PCCO are in the expected trivalent state at room temperature, the appearance of Pr^{4+} at $T < T_{\text{MI}}$ has been demonstrated by different groups using diverse experimental techniques.^{6,8} The process of intersite charge transfer between Pr and Co ions is reflected, among others, in the X-ray absorption spectra of Pr and Co atoms at different edges. At the Pr $M_{4,5}$ edges, a clear signature of Pr^{4+} is the enhancement and shift to higher energies of the C and D spectral features. The absorption cross section at the E and F features increases too. This evolution is absent in PSCO, which in combination with the already-mentioned spectral similarity to PCCO at 300 K suggests that there is no trace of tetravalent Pr ions in PSCO at low temperatures.

We carried out charge-transfer multiplet calculations²⁰ of the experimental X-ray absorption spectra plotted in Figure 2 to explore the effects of a hypothetical Pr^{4+} content in these cobaltites. Thus, in Figure 3a,b we show the calculated spectra at the Pr $M_{4,5}$ absorption edges for a Pr^{4+} -based oxide with a pseudocubic perovskite structure and a pure Pr^{3+} -based one. We note here that we included a significant charge transfer component in the Pr^{4+} cobaltite calculation in an attempt to simulate the experimental spectrum of PCCO.²¹ We therefore decided to label it as $\text{Pr}^{4+}_{\text{CT}}$. In this case, the initial and final states of the 3d XAS process can be described as a mixture of the $4f^1$ and $4f^2\bar{\downarrow}$ configurations and a mixture of the $3d^94f^2$ and $3d^94f^3\bar{\downarrow}$ configurations, respectively, where $\bar{\downarrow}$ stands for a hole in the valence band. The results of a pure Pr^{3+} -based compound calculation are also shown for comparison (Figure 3c). The parameter values used for every calculation are reported in ref 22. As empirically shown in a recent work,⁹ the experimental Pr $M_{4,5}$ (and Pr L_3) XAS spectra of PCCO at $T < T_{\text{MI}}$ can be reproduced as the weighted addition of the two latter components in a variable $\text{Pr}^{3+}:\text{Pr}^{4+}_{\text{CT}}$ ratio that is directly proportional to the temperature. In Figure 3d we show simulations of the PCCO spectra at 10 and 300 K following this method using the values derived in ref 9. The comparison to the low-temperature experimental spectra for PCCO and PSCO reinforces the idea of an absence of tetravalent Pr ions in the latter compound.

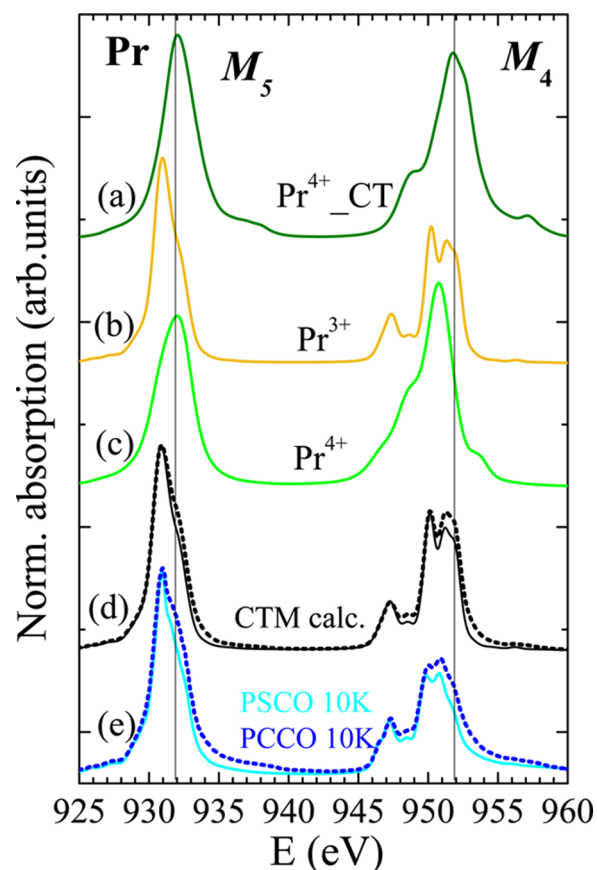


Figure 3. (a–c) Calculated Pr $M_{4,5}$ XAS spectrum of a Co-based perovskite containing only $\text{Pr}^{4+}_{\text{CT}}$ (charge transfer allowed) (green), Pr^{3+} (no charge transfer) (yellow), and Pr^{4+} (no charge transfer) (light green). (d) Comparison of a Pr^{3+} -based cobaltite multiplet calculation (black solid line) to the 85:15 weighted addition of calculated Pr^{3+} and $\text{Pr}^{4+}_{\text{CT}}$ spectra (black dotted line). (e) Comparison of the experimental spectra of $\text{Pr}_{0.50}\text{Sr}_{0.50}\text{CoO}_3$ (light-blue solid line) and $\text{Pr}_{0.50}\text{Ca}_{0.50}\text{CoO}_3$ (blue dotted line) measured at 10 K. Spectra have been vertically shifted for clarity.

XAS at the Pr L_3 edge (Figure 4) confirms our conclusions obtained from the soft X-ray regime on the stability of the Pr

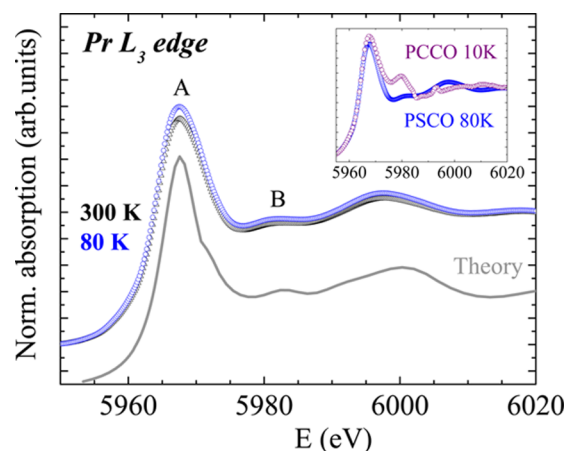


Figure 4. Experimental Pr L_3 -edge XAS spectrum of PSCO at room temperature (black Δ) and 80 K (blue \circ). The solid gray line corresponds to the calculated spectrum. The inset shows a comparison between PCCO and PSCO in low-temperature phases.

oxidation state. Let us note that the appearance of Pr^{4+} in PCCO leads to a noticeable enhancement of the B feature at T_{MI} (as can be seen in the inset). Regardless of temperature, the absorption cross section at ~ 5980 eV shows a local maximum due to multiple scattering of the photoelectron from ionized Pr atoms with the surrounding atomic environment (i.e., it has a structural origin). Nevertheless, its enhancement at $T < T_{\text{MI}}$ responds to the Pr^{4+} formation.⁸ This thermally modulated spectral evolution does not occur in PSCO, in agreement with the absence of Pr^{4+} derived from the analysis of XAS spectra shown in Figures 2 and 3. To gain insight into the Pr L_3 edge results, we also carried out X-ray absorption simulations based on the self-consistent real-space multiple scattering approach.²³ The simulations were performed employing the crystallographic *Imma* structure of PSCO at $T > T_S$.^{17,24,25} The theoretical spectrum obtained is plotted at the bottom of Figure 4, and it is in good agreement with the experimental spectra.

B. XAS at the Co $L_{2,3}$ and O K edges. We have so far looked for similarities with PCCO to resolve whether charge transfer involving Pr atoms takes place across T_S in PSCO. More common physical phenomena in cobalt oxides are Co spin-state transitions. We carried out XAS measurements at the Co $L_{2,3}$ edges to profit from the direct sensitivity to the electronic filling details of the valence orbitals. Figure 5 shows

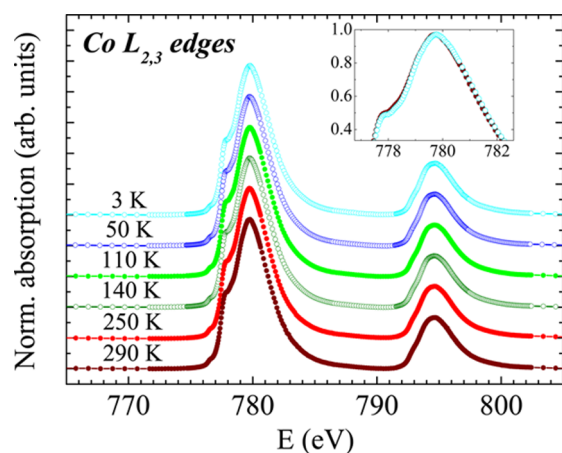


Figure 5. Experimental Co $L_{2,3}$ XAS spectra as a function of temperature for $\text{Pr}_{0.50}\text{Sr}_{0.50}\text{CoO}_3$. The inset shows details of the 290 K (red ●) and 3 K (blue ○) curves. Spectra have been vertically shifted for clarity.

the evolution of the Co $L_{2,3}$ XAS spectra of PSCO as a function of temperature between 3 and 290 K. Changes are minimal over the whole thermal range studied. In other words, there are no relevant variations in the occupation of the Co 3d states. In view of this and the results presented in section A, we cannot relate the mechanism driving the anomalous transition taking place at T_S to either a Pr-to-Co charge transfer or Co spin-state changes.

Pre-edge features in the O K edge X-ray absorption spectra are an alternative way to analyze the occupation of Co 3d states via hybridization to O 2p states. Figure 6 displays the temperature-dependent O K edge spectra for PSCO. We have also plotted the spectrum of PrCoO_3 at 10 K containing only Co^{3+} in the LS state ($t_{2g}^6e_g^0$, $S = 0$). We note the absence of changes with temperature in PSCO, similar as in the Co $L_{2,3}$ edge spectra. In addition, the comparison to the PCO reference spectrum is a strong indication of the existence of a large

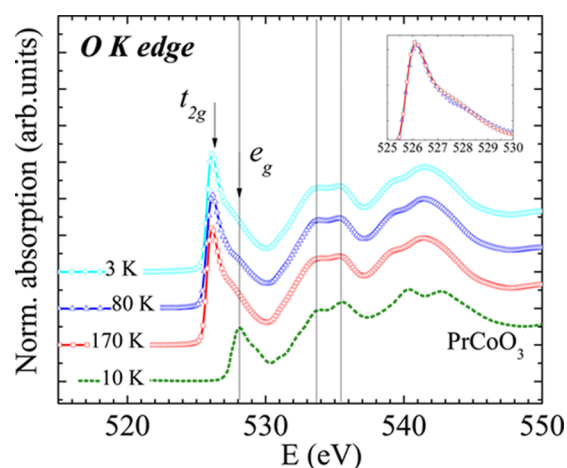


Figure 6. Experimental O K edge XAS spectra of $\text{Pr}_{0.50}\text{Sr}_{0.50}\text{CoO}_3$ at different temperatures. The experimental spectrum of PrCoO_3 (green dotted line) serves as a reference. The inset displays details of the pre-edge region of the PSCO spectra.

density of 3d t_{2g} empty states in Co ions for $\text{Pr}_{0.50}\text{Sr}_{0.50}\text{CoO}_3$. The temperature-dependent spectral weight ratio of empty t_{2g} and e_g states is characteristic of PCCO and similar Pr–Ca cobaltites.^{4,26} This allows us to remark that the electronic configuration of Co ions in PSCO is very different from that in PCCO at $T < T_{\text{MI}}$. In $\text{Pr}_{0.50}\text{Ca}_{0.50}\text{CoO}_3$, the insulating phase presents a coexistence of Co^{3+} ($3d^6 t_{2g}^6 e_g^0$, $S = 0$) and Co^{4+} ($3d^5 t_{2g}^5 e_g^0$, $S = 1/2$) ions, both in the LS state. This involves a scarcity of empty 3d states with t_{2g} symmetry in PCCO and helps to explain the large amplitude of PSCO O K edge prepeak features at ~ 528 eV.

CONCLUSIONS

We have presented a complete variable-temperature spectroscopic study of $\text{Pr}_{0.50}\text{Sr}_{0.50}\text{CoO}_3$, which presents an anomalous transition at $T_S \sim 120$ K. There is a noteworthy contraction of the average Pr–O bond length $\langle d_{\text{Pr-O}} \rangle^{\text{VIII}}$ at T_S , which suggests a large hybridization between Pr 4f and O 2p orbitals as a possible mechanism for the transition. However, unlike other similar cobaltites ($\text{Pr}_{0.50}\text{Ca}_{0.50}\text{CoO}_3$),^{4,8,9} we did not observe any Pr^{3+} to Pr^{4+} oxidation process across it after inspection of the XAS spectra at the Pr $M_{4,5}$ and Pr L_3 edges. Moreover, charge transfer multiplet simulations support our experimental results. Even though there is no valence change in Pr ions across T_S , they actively participate to catalyze the onset of this transition. This may be related to the strong Pr–O hybridization across T_S without charge transfer. In addition, we have observed a large density of free 3d states with t_{2g} symmetry in PSCO Co ions according to O K edge XAS. Thus, we can qualitatively talk in terms of an excited high-spin (HS) or intermediate-spin (IS) state, either pure or mixed with a small contribution from the low-spin configuration. We have also seen by inspection of the Co $L_{2,3}$ XAS spectra that the average spin state of Co is insensitive to temperature over the studied range. A plausible hypothesis for the Co spin state in PSCO is to have an equilibrated mixture of Co^{3+} ions in an IS or HS state, with Co^{4+} ions staying in an LS state or even an IS state as proposed for other cobaltites of the $(\text{Pr}_{1-y}\text{Ln}_y)_{1-x}\text{Ca}_x\text{CoO}_3$ family.²⁶ A large population of Co ions in an LS state at $T < 120$ K is unexpected because of the metallic character of PSCO at low temperatures. Further theoretical studies to better determine the spin state in $\text{Pr}_{0.50}\text{Sr}_{0.50}\text{CoO}_3$ would be desirable.

■ AUTHOR INFORMATION

Corresponding Author

*E-mail: jpadilla@icmab.es.

Notes

The authors declare no competing financial interest.

■ ACKNOWLEDGMENTS

We thank MICINN (Spanish Government) for financial support under Projects MAT2009-09308, MAT2012-38213-C02-02, and CSD2007-00041 (NANOSELECT). These experiments were performed on the BL29-BOREAS and BL22-CLÆSS beamline at ALBA Synchrotron and on ID08 at the ESRF with the collaboration of local staff and particularly A. Barla and E. Pellegrin. J.P.-P. gratefully acknowledges C. Piamonteze for her assistance with multiplet calculations and CSIC for a JAE-Predoc contract.

■ REFERENCES

- (1) Tsubouchi, S.; Kyômen, T.; Itoh, M.; Ganguly, P.; Oguni, M.; Shimojo, Y.; Morii, Y.; Ishii, Y. *Phys. Rev. B* **2002**, *66*, No. 052418.
- (2) Frontera, C.; García-Muñoz, J. L.; Llobet, A.; Aranda, M. A. G. *Phys. Rev. B* **2002**, *65*, No. 180405(R). Also see: Frontera, C.; García-Muñoz, J. L.; Carrillo, A. E.; Aranda, M. A. G.; Margiolaki, I.; Caneiro, A. *J. Solid State Chem.* **2003**, *171*, 349.
- (3) Maignan, A.; Caignaert, V.; Raveau, B.; Khomskii, D.; Sawatzky, G. *Phys. Rev. Lett.* **2004**, *93*, No. 026401. Also see: Frontera, C.; García-Muñoz, J. L.; Carrillo, A. E.; Aranda, M. A. G.; Margiolaki, I.; Caneiro, A. *Phys. Rev. B* **2006**, *74*, No. 054406.
- (4) Herrero-Martín, J.; García-Muñoz, J. L.; Kvashnina, K.; Gallo, E.; Subías, G.; Alonso, J. A.; Barón-González, A. J. *Phys. Rev. B* **2012**, *86*, No. 125106.
- (5) Barón-González, A. J.; Frontera, C.; García-Muñoz, J. L.; Blasco, J.; Ritter, C. *Phys. Rev. B* **2010**, *81*, No. 054427.
- (6) Hejtmanek, J.; Šantavá, E.; Knížek, K.; Maryško, M.; Jiráček, Z.; Naito, T.; Sasaki, H.; Fujishiro, H. *Phys. Rev. B* **2010**, *82*, No. 165107.
- (7) Knížek, K.; Hejtmanek, J.; Novák, P.; Jiráček, Z. *Phys. Rev. B* **2010**, *81*, No. 155113.
- (8) García-Muñoz, J. L.; Frontera, C.; Barón-González, A. J.; Valencia, S.; Blasco, J.; Feyerherm, R.; Dudzik, E.; Abrudan, R.; Radu, F. *Phys. Rev. B* **2011**, *84*, No. 045104.
- (9) Herrero-Martín, J.; García-Muñoz, J. L.; Valencia, S.; Frontera, C.; Blasco, J.; Barón-González, A. J.; Subías, G.; Abrudan, R.; Radu, F.; Dudzik, E.; Feyerherm, R. *Phys. Rev. B* **2011**, *84*, No. 115131.
- (10) Mahendiran, R.; Schiffer, P. *Phys. Rev. B* **2003**, *68*, No. 024427.
- (11) Leighton, C.; Stauffer, D. D.; Huang, Q.; Ren, Y.; El-Khatib, S.; Torija, M. A.; Wu, J.; Lynn, J. W.; Wang, L.; Frey, N. A.; Srikanth, H.; Davies, J. E.; Liu, K.; Mitchell, J. F. *Phys. Rev. B* **2009**, *79*, No. 214420.
- (12) Frey Huls, N. A.; Bingham, N. S.; Phan, M. H.; Srikanth, H.; Stauffer, D. D.; Leighton, C. *Phys. Rev. B* **2011**, *83*, No. 024406.
- (13) Troyanchuk, I. O.; Karpinskii, D. V.; Chobot, A. N.; Voitsekhovich, D. G.; Bobryanskii, V. M. *JETP Lett.* **2006**, *84*, 151.
- (14) Balagurov, A. M.; Bobrikov, I. A.; Pomjakushin, V. Y.; Pomjakushina, E. V.; Sheptyakov, D. V.; Troyanchuk, I. O. *JETP Lett.* **2011**, *93*, 263.
- (15) Hirahara, S.; Nakai, Y.; Miyoshi, K.; Fujiwara, K.; Takeuchi, J. J. *Magn. Magn. Mater.* **2007**, *310*, 1866.
- (16) Stauffer, D. D.; Leighton, C. *Phys. Rev. B* **2004**, *70*, No. 214414.
- (17) Padilla-Pantoja, J.; Barón-González, A. J.; Bozzo, B.; Blasco, J.; Ritter, C.; Herrero-Martín, J.; García-Muñoz, J. L. *Physica B*, in press; *J. Appl. Phys.*, **2014**, *115*, No. 17D721.
- (18) Thole, B. T.; van der Laan, G. *Phys. Rev. B* **1988**, *38*, 3158.
- (19) Thole, B. T.; van der Laan, G.; Fuggle, J. C.; Sawatzky, G. A.; Karnatak, R. C.; Esteve, J.-M. *Phys. Rev. B* **1985**, *32*, 5107.
- (20) Cowan, R. D. *The Theory of Atomic Structure and Spectra*; University of California Press: Berkeley, CA, 1981.
- (21) Hu, Z.; Kaindl, G.; Ogasarawa, H.; Kotani, A.; Felner, I. *Chem. Phys. Lett.* **2000**, *325*, 241.
- (22) Parameters employed (eV) for Pr^{3+} : $F_{dd} = 0.9$, $F_{pd} = 1.00$, $G_{pd} = 1.00$, $\Delta = 0.0$. For Pr^{4+} CT: $\Delta = 1.0$, $t = 0.8$ using the charge transfer mode. For pure Pr^{4+} : $F_{dd} = 0.95$, $F_{pd} = 1.00$, $G_{pd} = 1.00$, spin-orbit coupling = 0.95.
- (23) Ankudinov, A. L.; Ravel, B.; Rehr, J. J.; Conradson, S. D. *Phys. Rev. B* **1998**, *58*, 7565.
- (24) Balagurov, A. M.; Bobrikov, I. A.; Karpinsky, D. V.; Troyanchuk, I. O.; Pomjakushin, V. Y.; Sheptyakov, D. V. *JETP Lett.* **2008**, *88*, 531.
- (25) Parameters employed: Dirac-Hara + Hedin-Lundqvist and a cluster of radius 7.5 Å around Pr atoms.
- (26) Guillou, F.; Zhang, Q.; Hu, Z.; Kuo, C. Y.; Chin, Y. Y.; Lin, H. J.; Chen, C. T.; Tanaka, A.; Tjeng, L. H.; Hardy, V. *Phys. Rev. B* **2013**, *87*, No. 115114.